0026-895X/91/010079-06$03.00/0

MOLECULAR PHARMACOLOGY, 39:79-84

γ-Butyrolactone Antagonism of the Picrotoxin Receptor: Comparison of a Pure Antagonist and a Mixed Antagonist/Inverse Agonist

KATHERINE D. HOLLAND, KONG-WOO YOON, JAMES A. FERRENDELLI, D. F. COVEY, and STEVEN M. ROTHMAN

Departments of Pharmacology (K.D.H., J.A.F., D.F.C.), Neurology (J.A.F.), and Anatomy and Neurobiology (K.-W.Y., S.M.R.), Washington University School of Medicine, St. Louis, Missouri 63110

Received June 26, 1990; Accepted October 24, 1990

SUMMARY

Multiple receptors modulate the ion channel gated by the inhibitory neurotransmitter γ-aminobutyric acid (GABA). γ-Butyrolactones and γ-thiobutyrolactones are compounds that act at the picrotoxin recognition site on the GABA receptor complex as either agonists or inverse agonists, depending on the nature of the alkyl substituents. Here we have compared the effects of two γ-butyrolactones, α-ethyl-α-methyl-γ-butyrolactone (αEMGBL) and α-isopropyl-α-methyl-γ-butryolactone (αIMGBL), on GABA currents and inhibitory postsynaptic currents (IPSCs) in cultured, voltage-clamped, rat hippocampal neurons. αEMGBL also decreased the rate of IPSC decay without altering IPSC peak amplitude. At higher GABA concentrations (30 μM), αEMGBL has already been shown to block picrotoxin receptor agonists and inverse agonists. Thus, αEMGBL is a mixed antagonist/inverse agonist. In contrast to αEMGBL, αIMGBL had no effect on responses to either 0.5 or 30 μM GABA or on IPSCs, but it was able to block the effects of picrotoxin receptor agonists and inverse agonists. Therefore, αIMGBL is the first pure antagonist to be described for the picrotoxin receptor. The main conductance state of the GABA-gated channel probably has two or more open states, brief openings associated with binding of a single GABA molecule and longer openings due to the binding of two GABA molecules. We were able to simulate the results obtained with αEMGBL, using a computer model, by assuming that αEMGBL altered only the opening and closing rate constants for the monoliganded open channel of the GABA receptor. In addition to having site-selective actions, these results suggest that drugs modulating the GABA-linked chloride ionophore may be specific for the kinetic state of the GABA-gated channel.

Channels directly gated by ligands such as glutamate, GABA, and acetylcholine account for most of the fast excitatory and inhibitory synaptic potentials in the nervous system (1). Although these channels must have a binding site for their grating ligand, it has become clear that many channels have additional receptors for other molecules that modulate their opening. The GABA channel-receptor complex has been the most extensively characterized in this regard. It has regions that bind barbiturates, benzodiazepines, or picrotoxin (2). The benzodiazepine receptor is interesting because the ligands that bind to it either augment GABA responses, diminish GABA responses, or eliminate the responses produced by other benzodiazepines (3). Compounds with these properties have been labeled benzodiazepine agonists, inverse agonists, and antagonists, respectively.

This work was supported by the Seay Neuropharmacology Research Fellowship, the McDonnell Center for Cellular and Molecular Neurobiology, and National Institutes of Health Grants NS14834, NS19988, and GM07805.

Recently, a series of GBLs and TBLs that can act as agonists or inverse agonists at the picrotoxin receptor have been described (4–12). When GBLs and TBLs are alkylated in the β-position, the resulting compounds are highly convulsant and produce seizures that resemble those caused by picrotoxinin (4, 5). In contrast, when GBL and TBL are substituted in the α-position, and the β-position remains unsubstituted, the resulting compounds are usually anticonvulsant (5, 6). Receptor binding studies indicate that both convulsant and anticonvulsant GBLs and TBLs bind to the picrotoxin receptor (7–9). In addition, electrophysiological experiments have shown that alkyl-substituted GBLs and TBLs alter GABA-mediated currents in cultured neurons. Convulsant GBLs and TBLs diminish GABA responses, whereas an anticonvulsant TBL, αEMTBL (Fig. 1), augments GABA responses. These results are all consistent with the hypothesis that alkyl-substituted GBLs and TBLs act at the picrotoxin receptor as either agonists or inverse agonists (10–12). We had initially thought that

ABBREVIATIONS: GABA, γ-aminobutyric acid; GBL, γ-butyrolactone; TBL, γ-thiobutyrolactone; αEMGBL, α-ethyl-α-methyl-γ-butyrolactone; αIMGBL, α-isopropyl-α-methyl-γ-butyrolactone; IPSC, inhibitory postsynaptic current; HEPES, 4-(2-hydroxyethyl)-1-piperazineethanesulfonic acid; EGTA, ethylene glycol bis(β-aminoethyl ether)-*N,N,N′,N′*-tetraacetic acid; αEMTBL, α-ethyl-α-methyl-γ-thiobutyrolactone.

another α-substituted GBL, αEMGBL, was a picrotoxin antagonist, but we subsequently found that it had both inverse agonist and antagonist properties (10). In this paper we describe another GBL, αIMGBL, which is a pure picrotoxin antagonist. We compared the effects of αEMGBL and αIMGBL on GABA-induced currents and IPSCs in voltage-clamped rat hippocampal neurons. Using previously reported kinetic schemes for GABA receptor activation, we suggest a novel hypothesis that can account for the mixed properties of αEMGBL.

Experimental Procedures

Materials. The GBLs were synthesized using protocols that have been described in detail (4–6). αIMGBL was prepared by alkylation (methyl iodide and lithium diisopropyl amide in tetrahydrofuran) of the known compound α-isopropyl-γ-butyrolactone (13) and had the expected analytical and spectroscopic properties. Unless noted otherwise, all other reagents were purchased from Sigma Chemical Co. (St. Louis, MO).

Tissue culture. Hippocampal neurons obtained from 1-day-old rat pups were grown using methods almost identical to those described by Huettner and Baughman (14). After incubation in 1 mg/ml papain, gentle trituration, and centrifugation, 2.5×10^5 cells were plated onto 35-mm culture dishes. The dishes had been preplated with cortical glia and contained minimal essential medium and 10% Nu Serum (Collaborative Research). After 3–5 days *in vitro*, glial division was inhibited by 15 μg/ml fluorodeoxyuridine and 35 μg/ml uridine. Physiology experiments were done with cultures at least 10 days old.

Electrophysiology. Neurons were voltage clamped at −60 mV with a commercial amplifier (Dagan), using the whole-cell recording technique described by Hamill and colleagues (15). Our extracellular solution included (in mM): 140 NaCl, 10 Na-HEPES, 3 KCl, 4 $MgCl_2$, and 5.5 glucose. The patch pipettes contained (in mM): 130 potassium acetate, 10 KCl, 10 Na-HEPES, 2 MgATP, and 1.1 EGTA. For experiments with 0.5 μM GABA, the solution was changed to contain 140 mM KCl, to amplify the effects of the low GABA concentration. With both pipette solutions, GABA gave inward currents at a holding potential of −60 mV. For experiments on IPSCs, the intracellular solution contained (in mM): 138 potassium isothionate and 2 KCl. IPSCs were then outward at −60 mV and easily distinguished from inward excitatory postsynaptic currents. GABA responses were examined by local application of GABA for 100 msec, alone or with other drugs, in a solution identical to the extracellular bath (16).

IPSCs were examined by stimulating one neuron via a bridge amplifier while recording from a nearby cell in voltage clamp. Monosynaptic inhibitory connections were found in about 50% of successful simultaneous impalements. These were reduced by bicuculline and were insensitive to the application of 6-cyand-7-nitroquinoxaline-2,3-dione (CNQX), an antagonist at glutamate receptors (17). IPSCs were recorded in normal extracellular solution, which was subsequently exchanged for a solution that contained the test drug. Peak amplitude, decay time, and charge transfer of IPSCs were measured before, during, and after drug exposure.

All physiological data was digitized and stored on disc for analysis (pClamp). In order to compensate for current variability as a function of neuron size, GABA dose-response curves were normalized to responses produced by a fixed concentration of GABA. For GABA dose-response curves from 10 μM to 1 mM, currents were normalized to 100 μM GABA and, for GABA concentration-response curves obtained at ≤10 μM GABA, all points were normalized to responses to 10 μM GABA. Concentration-response curves were fit by probit analysis and Hill plots were fit by linear regression analysis.

Results

The cells used in these studies had resting membrane potentials of −58 ± 7 mV (mean ± 1 SD; $n = 166$); the typical input resistances ranged from 90 to 800 MΩ and averaged 276 ± 42 MΩ. Applications of 30 μM GABA for 100 msec, spaced 30 sec apart, consistently produced currents of similar magnitude. When the magnitudes of the currents produced by varying concentrations of GABA were normalized to the response produced by 100 μM GABA, a sigmoidal dose-response curve was obtained (Fig. 2A). The concentration of GABA that produced half-maximal response was 50 ± 5 μM (mean ± SE) and the responses to GABA were saturated at 300 μM. Between 10 μM and 1 mM GABA, the Hill slope was 1.8, similar to the value found by others using whole-cell recording (16, 18). However, between 1 and 10 μM, the Hill slope declined to 1.6.

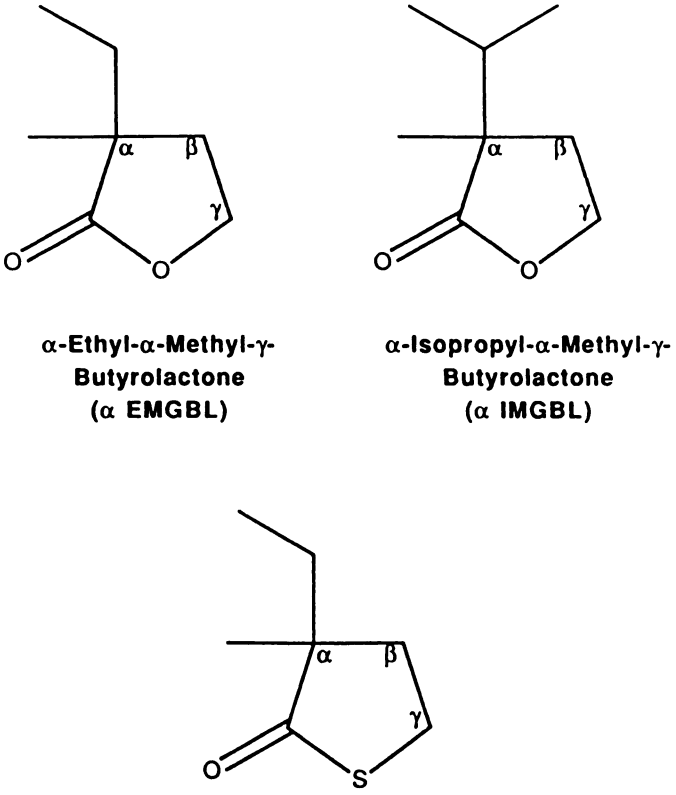

Fig. 1. Structures of αEMGBL, αIMGBL, and αEMTBL.

The effect of αEMGBL on GABA currents (10 mM) was dependent upon GABA concentration (Fig. 2B). It potentiated responses to low GABA concentrations (≤10 μM) but did not alter currents produced by GABA concentrations of >10 μM. For example, in the presence of αEMGBL (10 mM) the response to 1 μM GABA was nearly doubled, whereas the response to 10 μM GABA with 10 mM αEMGBL was identical to that of GABA alone. The Hill slope of the GABA dose-response curve below 10 μM GABA dropped from 1.6 to 1.2 in the presence of 10 mM αEMGBL ($p < 0.01$, Student's t test).

As has been reported previously (10, 11), αEMTBL potentiated responses produced by focal application of 30 μM GABA (Fig. 3A). The potentiation of GABA responses by 300 μM αEMTBL was almost completely eliminated when αEMTBL was coapplied with αEMGBL. αEMGBL can also diminish the action of 30 μM picrotoxinin, which alone reduced GABA currents by about 50% (10).

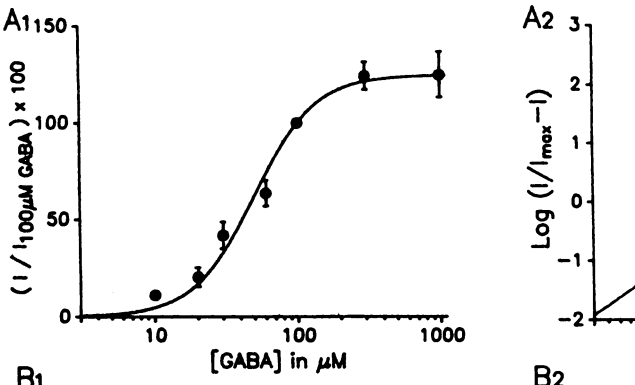

Fig. 2. GABA concentration-response curves and Hill plots. A, Curve for GABA concentrations ranging from 10 μM to 1 mM (*1*) translates to a Hill plot (*2*) with a slope of 1.8. The actual points on the concentration-response curve are averages from at least seven neurons. B, Curves for GABA concentrations between 1 and 10 μM in the absence and presence of 10 mM αEMGBL (*1*). The lower concentrations, but not 10 μM, were potentiated by αEMGBL. The maximum current obtained in the GABA concentration-response curve (*A1*) was used in all three Hill plots, which were calculated from the responses of individual cells.

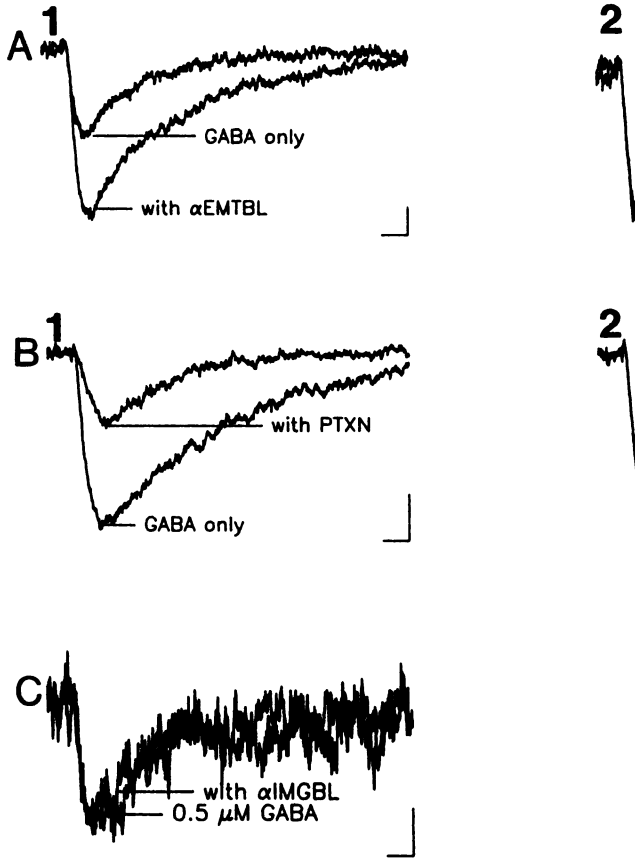

Fig. 3. Action of αEMGBL and αIMGBL on responses produced by application of GABA. A, αEMTBL (300 μM) potentiates responses to 30 μM GABA (*1*), and this is blocked by the application of 3 mM αIMGBL (*2*). B, Picrotoxinin (*PTXN*) (300 μM) inhibits responses to 30 μM GABA (*1*), and this is blocked by the application of 3 mM αIMGBL (*2*). C, αIMGBL (3 mM) has no effect on responses to either 30 μM GABA (not shown) or 0.5 μM GABA. Calibrations for A and B, 20 pA by 250 msec; for C, 10 pA by 250 msec.

Like αEMGBL, αIMGBL had no effect on responses to 30 μM GABA (Table 1). It prevented the potentiation of responses to 30 μM GABA produced by αEMTBL (Table 1; Fig. 3A) and the inhibition of responses to 30 μM GABA produced by 30 μM picrotoxinin (Table 1; Fig. 3B). However, unlike αEMGBL, αIMGBL did not alter responses to low concentrations of GABA (0.5 μM) (Table 1; Fig. 3C).

Neither αEMGBL nor αIMGBL had direct effects on membrane potential, current-voltage plots, GABA reversal potentials, or action potentials.

TABLE 1
Action of αIMGBL on GABA currents and IPSCs

Drug combinations[a]	GABA current
	% of control
GABA (30 μM) + αEMTBL	196 ± 10 (22)[b]
GABA (30 μM) + αEMTBL + αIMGBL	118 ± 8 (10)[c]
GABA (30 μM) + picrotoxinin	44 ± 4 (19)
GABA (30 μM) + picrotoxinin + αIMGBL	88 ± 8 (11)[c]
GABA (30 μM) + αIMGBL	95 ± 7 (9)
GABA (0.5 μM) + αIMGBL	104 ± 6 (8)
Effect of αIMGBL on IPSCs	**IPSC**
	% of control
Peak amplitude	99 ± 5 (5)
τ_{IPSC}[d]	111 ± 6 (5)
Q_{IPSC}[e]	105 ± 7 (5)

[a] Drug concentrations: 300 μM αEMTBL, 3 mM αIMGBL, and 30 μM picrotoxin.
[b] Number of observations are given in parentheses.
[c] $p < 0.001$, compared with response without α-IMGBL, Student's t test.
[d] Decay time constant of IPSC.
[e] IPSC magnitude integrated over duration of IPSC.

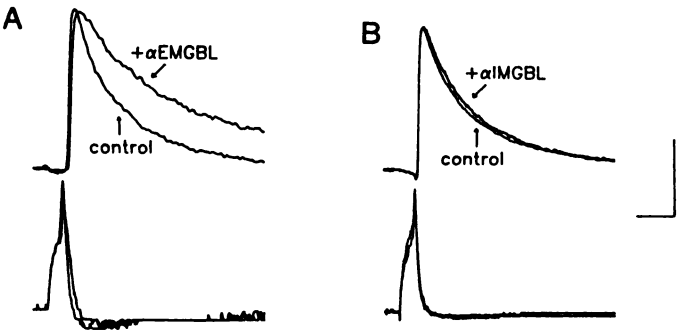

Fig. 4. Comparison of the effects of αEMGBL and αIMGBL on IPSCs. In each part, the *top traces* are IPSCs elicited by stimulation of a nearby neuron and the *bottom traces* are the presynaptic action potentials. A, 10 mM αEMGBL prolongs IPSC duration without altering IPSC peak amplitude. B, 3 mM αIMGBL does not effect IPSC duration or amplitude. The presynaptic action potentials were sometimes followed by autaptic IPSPs, which were variably modulated by the different lactones. This can be seen in presynaptic traces A. Calibrations for IPSCs, 100 pA by 25 msec (A) or 170 pA by 25 msec (B), for action potentials, 45 mV.

Because the IPSCs in our cultured neurons are produced by synaptically released GABA, we examined the effects of 3 mM αIMGBL on IPSCs. IPSC peak amplitude was 99 ± 5% of control (n = 5; not significant), and the IPSC time constant was 111 ± 6% of control (not significant) and the IPSC charge transfer was 105 ± 7% of control (not significant) in the presence of αIMGBL (Table 1; Fig. 4). The failure of αIMGBL to influence the IPSC time course is in marked contrast to αEMGBL (Fig. 4) (10).

Discussion

The picrotoxin receptor is thought to be the site of action of several convulsant and anticonvulsant GBLs and TBLs (7–12). Convulsant GBLs and TBLs act as agonists at this receptor. That is, they inhibit responses to the inhibitory neurotransmitter GABA in voltage-clamped neurons (10, 12). In contrast, anticonvulsant butyrolactones potentiate the actions of GABA and are picrotoxin receptor inverse agonists (10, 11). Here we have described the effects of αIMGBL, which had no effect on currents induced by either low or high GABA concentrations and did not alter IPSC amplitude or duration. However, αIMGBL was able to block the action of a picrotoxin receptor agonist (picrotoxinin) and a picrotoxin receptor inverse agonist (αEMTBL). Thus, αIMGBL appears to act as a pure antagonist at the picrotoxin receptor and is the first such compound to be identified.

The effects of the other GBL studied here, αEMGBL, were initially paradoxical. It prolonged IPSCs but did not increase or noticeably prolong responses to 30 μM GABA. This finding may be explained by recent patch-clamp observations on the kinetics of the high conductance GABA channel-receptor complex (19–23), which suggest that the channel may enter a short-lived open state after the GABA receptor binds a single GABA molecule; entry into other open states requires the binding of a second GABA molecule. Thus, rapid application of GABA or low GABA concentration would enhance the relative contribution of the monoliganded open state to the total GABA current. If αEMGBL increased the frequency of transitions into the monoliganded open state (or diminished its rate of closing), then it should selectively augment currents produced by low concentrations of GABA. This prediction was verified when αEMGBL was applied with a very low GABA concentration (0.5 μM). The peak GABA current was doubled under these conditions.

Using a model based on GABA single-channel data of others (20), we found that we could simulate our experimental data (TUTSIM; Applied i, Palo Alto). We assume that αEMGBL only alters the "opening" or "closing" rate constants for entering or leaving the monoliganded open channel and that the following scheme describes GABA (G) binding to its receptor (R) and opening channels (*):

$$\begin{array}{ccc} G + R \underset{k_2}{\overset{k_1}{\rightleftharpoons}} GR & + & G \underset{k_6}{\overset{k_5}{\rightleftharpoons}} G_2R \\ k_3 \downarrow\uparrow k_4 & & k_7 \downarrow\uparrow k_8 \\ GR^* & & G_2R^* \underset{k_{10}}{\overset{k_9}{\rightleftharpoons}} G_2R'^* \end{array}$$

This is identical to scheme III of Weiss and Magleby (20), except that we make the binding steps explicit. This is also one of the possible schemes suggested by Macdonald *et al.* (21) and is similar to the models of Bormann and Clapham (22) and Mathers and Wang (23), except for the existence of the third open state. The rate constants (k_1–k_{10}) from a single patch (no. 1) from Weiss and Magleby (20) were also used. The effect of αEMGBL was simulated by reductions in k_3 and k_4 from 66.4 sec^{-1} to 13 sec^{-1} and 2810 sec^{-1} to 150 sec^{-1}, respectively. αEMGBL had virtually no detectable effect on the peak and decay of a simulated 30 μM, 100-msec GABA application (Fig. 5). A simulated 0.5 μM, 100-msec GABA application was potentiated by approximately 100% (Fig. 5B). The effect of αEMGBL on a simplified model of an IPSC (Fig. 5C) also closely resembled our experimental results, although it was not possible to duplicate exactly the time course of exogenous GABA currents or IPSCs, owing to uncertainties about transmitter concentration and persistence and the contribution of other conductance states to the IPSC. Thus, when we made a large reduction in the closing rate and a small reduction in the opening rate, we could largely duplicate our data with no other rate constant changes.

Data obtained from the Hill plots are also consistent with the hypothesis that αEMGBL increases the contribution of the monoliganded open state to the total GABA current. Between 10 μM and 1 mM GABA the Hill slope was 1.8, but between 1

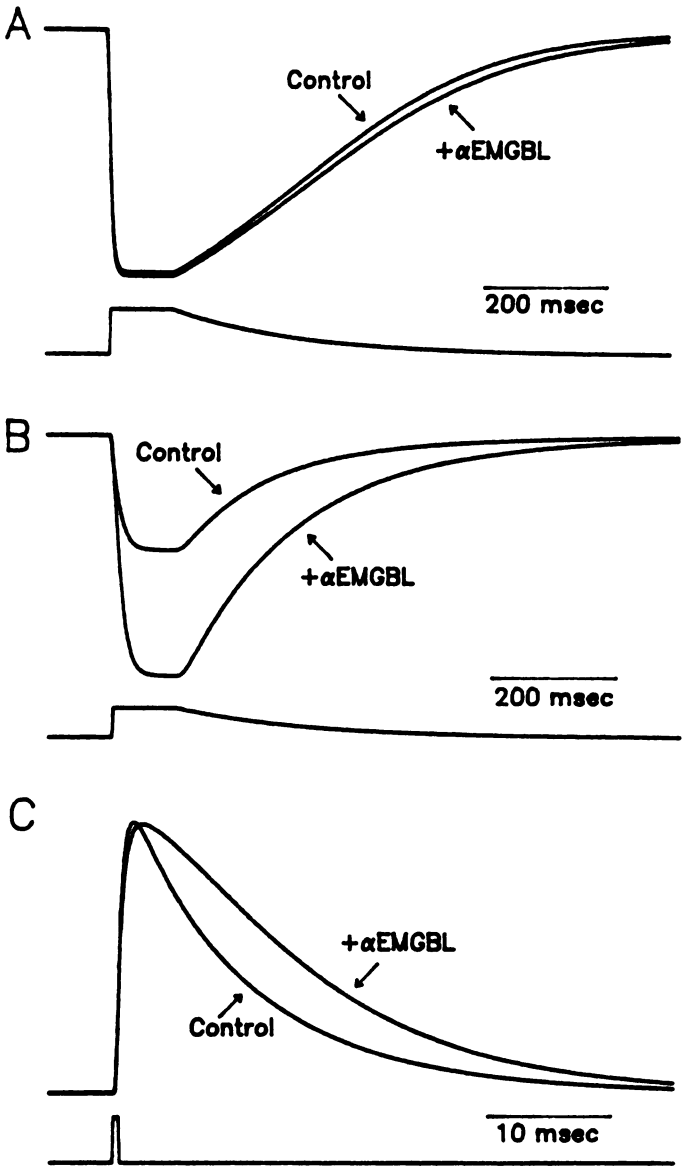

Fig. 5. Simulation of GABA currents and IPSCs. A, Whole-cell currents are produced by a simulated application of 30 μM GABA. The simulation assumes that the extracellular GABA concentration stays at 30 μM for 100 msec and then decays exponentially with a time constant of 5 sec^{-1} when k_3 and k_4 are reduced by αEMGBL. The peak GABA response is virtually unaffected, whereas the decay is only slightly prolonged. This decreased decay rate would be very difficult to detect experimentally. B, When the GABA concentration in the simulation is reduced to 0.5 μM, αEMGBL doubles the peak GABA current. In both A and B, the current flattens at the peak because the simulated constant GABA concentration allows the reaction to come to equilibrium. C, An IPSC is simulated as a 0.5-msec step of 50 μM GABA. When k_3 and k_4 are reduced, the rise of the IPSC is only slightly reduced but the decay rate is markedly prolonged. In A–C, the vertical scale is current in arbitrary units. *Bottom line* of each figure, time course of the GABA application, with concentration not drawn to scale.

and 10 μM the Hill slope declined to 1.6, consistent with an increased contribution of monoliganded channels to total GABA current at low concentration. More interestingly, over this range αEMGBL potentiated the GABA current and further reduced the Hill slope to 1.2. This result would be anticipated if αEMGBL favored the opening of monoliganded channels.

However, this hypothesis should be interpreted cautiously. The simulation based on the observations of Weiss and Magleby cannot prove its validity, because other combinations of rate constant alterations could also fit our data. In addition, this model is likely incomplete, because it fails to consider other properties of the channel, such as desensitization. The reduction in Hill slope produced by αEMGBL is also not absolute proof that the compound favors the monoliganded open state, because the assumptions that enter into the derivation of the Hill equation are not completely applicable to channel kinetics. Nevertheless, both the simulation and the Hill plot data together provide strong support for the idea that αEMGBL has its predominant effect on the monoliganded GABA open state, although this does not exclude effects on other states.

The concept of "state selectivity" now has some precedent, at least for the GABA receptor channel, because Macdonald and colleagues (24) have recently suggested an analogous mechanism to explain barbiturate enhancement of GABA currents. Their data, obtained from single-channel measurements, suggest that barbiturates selectively enhance entry into one of the diliganded open states. In contrast, we propose that aEMGBL increases the duration of the monoliganded open state without affecting the rate of GABA binding to its receptor. The latter is consistent with previous experiments that failed to show any enhancement of [^{3}H]muscimol affinity by αEMGBL (9). Because complicated gating schemes have been suggested for additional agonist-gated channels (25), the possibility of state-selective effects of other drugs and natural modulatory substances will have to be considered.

Two main conclusions may be drawn from our results. First, this is the first demonstration of a pure picrotoxin receptor antagonist (αIMGBL). Now, agonists, inverse agonists, and antagonists have been described for both the benzodiazepine (3) and picrotoxin receptors (9, 10, 26, 27). Any structure proposed for the GABA channel-receptor complex in the future will have to account for this type of modulation at two separate sites (28). Second, our results emphasize the potential importance of kinetic models in elucidating drug effects on whole-cell currents. Our results would be difficult to explain had we assumed that GABA channels open to only one state after binding two GABA molecules, the traditional view based on Hill plots employing long GABA applications at concentrations of >10 μM (16, 22). The gating schemes suggested by four groups studying single GABA channels (18–21) provide a ready and plausible explanation for our results. They indicate that the monoliganded channel may contribute a substantial component to the whole-cell GABA current at low GABA concentrations or when GABA is applied briefly. This latter condition likely holds for the inhibitory synaptic currents, which are prolonged by αEMGBL but not αIMGBL.

Acknowledgments

We would like to thank Dr. Jeanne Nerbonne for help with the current simulations, Drs. Nerbonne, Jonathan Cohen, Robert Macdonald, and Joe Henry Steinbach for critique of earlier drafts of the manuscript, Nancy Lancaster for culture preparation, and Deborah Howard for secretarial help.

References

1. Iversen, L. L. Amino acids and peptides: fast and slow chemical signals in the nervous system. *Proc. R. Soc. Lond. B* **221**:245–260 (1984).
2. Bormann, J. Electrophysiology of $GABA_A$ and $GABA_B$ receptor subtypes. *Trends Neurosci.* **11**:112–116 (1988).
3. Polc, P., E. P. Bonetti, R. Schaffner, and W. Haefley. A three state model of the benzodiazepine receptor explains the interactions between the benzodiazepine antagonist Ro 15-1788, benzodiazepine tranquilizers, β-carbolines, and phenobarbitone. *Naunyn-Schmiedeberg's Arch. Pharmacol.* **15**:133–137 (1982).
4. Klunk, W. E., D. F. Covey, and J. A. Ferrendelli. Comparison of epileptogenic

properties of unsubstituted and β-alkyl substituted γ-butyrolactones. *Mol. Pharmacol.* **22**:431–437 (1982).
5. Levine, J. A., J. A. Ferrendelli, and D. F. Covey. Alkyl-substituted thiolo-, thiono-, and dithio-γ-butyrolactones: new classes of convulsant and anticonvulsant agents. *J. Med. Chem.* **29**:1996–1999 (1986).
6. Klunk, W. E., D. F. Covey, and J. A. Ferrendelli. Anticonvulsant properties of α, γ, and α,γ-substituted γ-butyrolactones. *Mol. Pharmacol.* **22**:438–443 (1982).
7. Weissman, B. A., T. R. Burke, K. C. Rice, and P. Skolnick. Alkyl-substituted γ-butyrolactones inhibit [^{35}S]TBPS binding to a GABA linked chloride ionophore. *Eur. J. Pharmacol.* **105**:195–196 (1984).
8. Levine, J. A., J. A. Ferrendelli, and D. F. Covey. Convulsant and anticonvulsant *gamma*-butyrolactones bind at the picrotoxinin/*t*-butylbicyclophosphorothionate (TBPS) receptor. *Biochem. Pharmacol.* **23**:4187–4190 (1985).
9. Holland, K. D., A. C. McKeon, D. F. Covey, and J. A. Ferrendelli. Binding interactions of convulsant and anticonvulsant γ-butyrolactones and γ-thiobutyrolactones with the picrotoxin receptor. *J. Pharmacol Exp. Ther.*, in press.
10. Holland, K. D., J. A. Ferrendelli, D. F. Covey, and S. M. Rothman. Physiological regulation of the picrotoxin receptor by γ-butyrolactones and γ-thiobutyrolactones in cultured hippocampal neurons. *J. Neurosci.* **10**:1719–1727 (1990).
11. Baker, K., J. Yang, D. F. Covey, D. B. Clifford, and C. F. Zorumski. α-Substituted thiobutyrolactones potentiate GABA current in voltage-clamped chick spinal cord neurons. *Neurosci. Lett.* **87**:133–138 (1988).
12. Clifford, D. B., K. Baker, J. Yang, D. F. Covey, and C. F. Zorumski. Convulsant *gamma*-butyrolactones block GABA currents in cultured chick spinal cord neurons. *Brain Res.* **484**:102–110 (1989).
13. Kendall, M., and R. J. Wells. Absolute configuration of 2- and 3-isopropyl-γ-butyrolactone. *Aust. J. Chem.* **27**:2293–2295 (1974).
14. Huettner, J. E., and R. W. Baughman. Primary culture of identified neurons from the visual cortex of postnatal rats. *J. Neurosci.* **6**:3044–3060 (1986).
15. Hamill, O. P., A. Marty, E. Neher, B. Sakmann, and F. J. Sigworth. Improved patch-clamp techniques for high resolution current recordings from cells and cell-free membrane patches. *Pfluegers Arch.* **391**:85–100 (1981).
16. Choi, D. W., and G. D. Fischbach. GABA conductance of chick spinal cord and dorsal root ganglion neurons in cell culture. *J. Neurophysiol.* **45**:605–620 (1981).
17. Honore', T., S. N. Davies, J. Krejer, G. J. Fletcher, P. Jacobsen, D. Lodge, and F. E. Nielsen. Quinoxalinediones: potent competitive non-NMDA glutamate receptor antagonists. *Science (Washington D. C.)* **241**:701–703 (1988).
18. Dichter, M. A. Physiological identification of GABA as the inhibitory transmitter for mammalian cortical neurons in cell culture. *Brain Res.* **190**:111–121 (1980).
19. Rothman, S. M., and M. Samaie. Physiology of excitatory synaptic transmission in cultures of dissociated rat hippocampus. *J. Neurophysiol.* **54**:701–713 (1989).
20. Weiss, D. S., and K. L. Magleby. Gating scheme for single GABA-activated Cl^- channels determined from stability plots, dwell-time distributions, and adjacent-interval durations. *J. Neurosci.* **9**:1314–1324 (1989).
21. Macdonald, R. L., C. J. Rogers, and R. E. Twyman. Kinetic properties of the $GABA_A$ receptor main conductance state of mouse spinal cord neurones in culture. *J. Physiol. (Lond.)* **410**:479–499 (1989).
22. Bormann, J., and D. E. Clapham. γ-Amino-butyric acid receptor channels in adrenal chromaffin cells: a patch clamp study. *Proc. Natl. Acad. Sci. USA* **82**:2168–2172 (1985).
23. Mathers, D. A., and Y. Wang. Effect of agonist concentration on the lifetime of GABA-activated membrane channels in spinal cord neurons. *Synapse* **2**:627–632 (1988).
24. Macdonald, R. L., C. J. Rogers, and R. E. Twyman. Barbiturate regulation of the kinetic properties of the $GABA_A$ receptor channel of mouse spinal neurones in culture. *J. Physiol. (Lond.)* **417**:483–500 (1989).
25. Jackson, M. B. Dependence of acetylcholine receptor channel kinetics on agonist concentration in cultured mouse muscle fibers. *J. Physiol. (Lond.)* **397**:555–583 (1988).
26. Ticku, M. K., and R. W. Olsen. Interaction of barbiturates with dihydropicrotoxinin binding sites related to the GABA receptor-ionophore system. *Life Sci.* **22**:1643–1652 (1978).
27. Leed-Lundberg, F., A. Snowman, and R. W. Olsen. Perturbation of benzodiazepine receptor binding by pyrazolopyridines involves picrotoxinin/barbiturate receptor sites. *J. Neurosci.* **1**:471–477 (1981).
28. Pritchett, D. B., H. Sontheimer, B. D. Shivers, S. Ymer, H. Kettenmann, P. R. Schofield, and P. H. Seeburg. Importance of a novel $GABA_A$ receptor subunit for benzodiazepine pharmacology. *Nature (Lond.)* **338**:582–585 (1989).

Send reprint requests to: Dr. James A. Ferrendelli, Department of Neurology and Neurosurgery, Box 8111, Washington University School of Medicine, 660 S. Euclid Ave., St. Louis, MO 63110.